# Comparison of Stability Criteria for Rotor Levitated by Active Magnetic Bearing

KANEMITSU,Yoichi, YONG,Xiao-Bing, KIJIMOTO,Shinya and MATSUDA,Koichi
*Faculty of Engineering, Kyushu University*
*Moto-oka, NIshi-ku, Fukuoka, 819-0395,JAPAN*
*kanemitu@mech.kyushu-u.ac.jp*

***Abstract* – In this paper, a phase margin, a gain margin, a sensitivity function, a maximum singular value of sensitivity function matrix and a damping ratio are taken up as indices which evaluate the stability margin of a rotor levitated by active magnetic bearings. The definition of the stability margin in this research is how far away the gain margin, the phase margin and the reciprocal number of the sensitivity function are from the critical point (-1 ,j0) in a polar plot. The stability margin distance is proposed to unify above-mentioned indices. We have estimated stability of a rotor-AMB system by these five indices and investigated relations among the indices.**

***Index Terms* – Stability criteria, Maximum singular value, Sensitivity function, Phase margin, Gain margin**

## Ⅰ. INTRODUCTION

An active magnetic bearing (AMB) is made of an electromagnet and a controller. A magnetizing current in the magnet is changed according to a gap between the bearing and a supported rotor and then the magnetizing pull from electromagnet levitates the rotor without contact. Therefore control system stability is a very important property for a magnetic bearing system which consisted of rotor, electromagnet and controller from a viewpoint which raises the operation reliability of the rotating machine which uses magnetic bearings.

ISO has adopted standardization on vibration of Active Magnetic Bearing as a new work item of ISO/TC108/SC2 in August 1993. JSME ATS10-25 Technical Section for Standardization on Active Magnetic Bearing is preparing a series of ISO drafts on terminology, vibration criteria and stability criteria for AMB equipped rotating machinery[1][2][3][4].

We have joined the JSME ATS10-25 Technical Section and carried out some related researches.

In this paper, a phase margin, a gain margin, a sensitivity function, a maximum singular value of sensitivity function matrix and a damping ratio are taken up as indexes by which the stability of a magnetic bearing system are evaluated. We have estimated stability of a rotor-AMB system by these five indices and investigated relations among the indices.

## Ⅱ. DEFINITION OF STABILITY MARGIN IN ISO-14839-3

ISO/DIS-14839-3 "Mechanical Vibration of rotating machinery equipped with active magnetic bearings-- Part3: Evaluation of stability margin" is under deliberation at present and has in the vote stage of FDIS, and goes into effect as formal ISO soon. The maximum gain (Peak sensitivity) of sensitivity functions is to be adopted as an evaluation index in this ISO draft standard. The relation between the stability valuation zone and the zone limit values is further determined described in the ISO final draft as Table 1.

Table 1 Peak sensitivity at zone limits

| Zone | Peak sensitivity | |
|---|---|---|
| | Level | Factor |
| A/B | 9.5dB | 3 |
| B/C | 12dB | 4 |
| C/D | 14dB | 5 |

The definition of Zone A, B, C and D is the same as that of other ISO vibration standards.

The gain margin and the phase margin are used to evaluate a control system stability in adjustment of conventional control apparatus. The damping ratio is evaluating the stability of a vibration system and the maximum singular value of the sensitivity function matrix is the index of a $H_\infty$ robust control design method.

We take up the gain margin, the phase margin, the damping ratio, the maximum gain (Peak sensitivity) of a sensitivity function and the maximum singular value of the sensitivity function matrix as the indexes of system stability margin in the study. It is investigated with a rotor supported by small active magnetic bearings what kind of relations they have.

* This work is partially supported by JSPS Grant-in-Aid for Scientific Research #17560210 to Y.Kanemitsu

## Ⅲ. DEFINITION OF STABILITY MARGIN DISTANCE

A vector locus of the open-loop transfer function of a control system is drawn on a Gauss plane and the phase margin and the gain margin are given by intersection between the vector locus and the real axis or a unit circle. The stability of the SISO control system is conventionally evaluated from the magnitude of the gains

Such gain is given as a non-dimensional distance from a critical point (-1, j0) of a Gauss plane.

The definition of the stability margin in this research is how far away the gain margin, the phase margin and the reciprocal number of the sensitivity function are from the critical point (-1 ,j0) in polar plot.

The stability margin distance (Distance Margin) $L$ is proposed to unify these relations in following explanations. The Polar diagram of the open loop transfer function is shown in Figure 1. A gain margin $g_m$ expresses a distance OA, and a phase margin $\phi_m$ expresses a phase angle <BOC. A distance from the critical point (-1, j0) is substituted for these quantities.

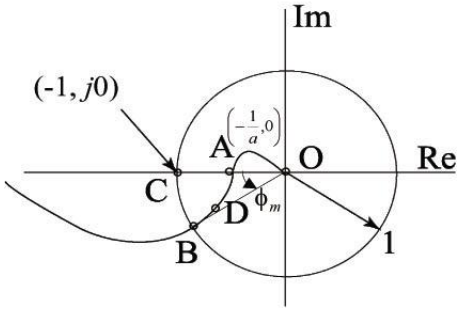


Figure 1 Stability Margin Distance

These distances are compared with the distance which is the reciprocal number of the sensitivity function in the same condition by following replacements.

The gain margin is given as follows:

$$g_m = 20\log_{10}\left(\frac{1}{\mathrm{OA}}\right) \tag{1}$$

Then the stability margin distance $L_{gm}(=\mathrm{CA})$ for the gain margin is calculated by a following equation:

$$L_{gm} = \mathrm{CA} = 1 - \mathrm{OA} = 1 - 10^{-gm/20} \tag{2}$$

On the other hand, the stability margin distance $L_{pm}$ for the phase margin can be shown with CB. Because $\mathrm{OC} = 1$ , $\mathrm{CB} = \mathrm{OC} \times \phi_m$ , the stability margin distance $L_{pm}(=\mathrm{CB})$ for the phase margin is

$$L_{pm} = \mathrm{CB} = \phi_m \tag{3}$$

The reciprocal number of the sensitivity function can be shown by the CD again in case of SISO, the stability margin distance $L_{ss}$ can be given as follows using maximum value $S_{\max}$ of sensitivity function $S(j\omega)$:

$$L_{ss} = \mathrm{CD} = \frac{1}{S_{\max}}, \quad S_{\max} = \max_{\omega}\left(\left|S(j\omega)\right|\right) \tag{4}$$

Four sets of active magnetic bearings should be employed to support a rotating shaft, but a decentralized control system is adopted for the rotor-AMB control system in many cases rather than a centralized control system. However actual rotor-AMB system has 4 inputs (4 proximity sensors) and 4 outputs (4 electromagnets), then is a MIMO system shown in Figure 2.

Adding sinusoidal sweep signals $(w_{x1}, w_{y1}, w_{x2}, w_{y2})$ to outputs of the proximity sensor outputs $(x_1, y_1, x_2, y_2)$, we can estimate the open loop transfer function matrix $\boldsymbol{G}(j\omega)$ and the sensitivity function matrix $\boldsymbol{S}(j\omega)$ of the rotor-AMB as a MIMO system as Equation(5)(6).

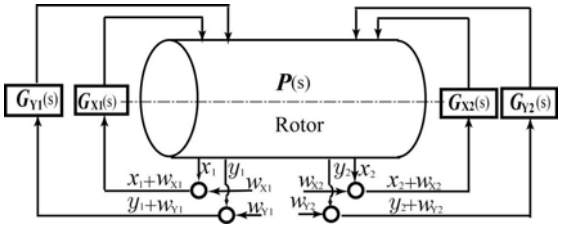


Figure 2 Block diagram of MIMO rotor-AMB system

$$\boldsymbol{G}(j\omega) = \begin{bmatrix} \frac{x_1}{w_{X1}+x_1} & \frac{y_1}{w_{X1}+x_1} & \frac{x_2}{w_{X1}+x_1} & \frac{y_2}{w_{X1}+x_1} \\ \frac{x_1}{w_{YL}+y_1} & \frac{y_1}{w_{YL}+y_1} & \frac{x_2}{w_{YL}+y_1} & \frac{y_2}{w_{YL}+y_1} \\ \frac{x_1}{w_{X2}+x_2} & \frac{y_1}{w_{X2}+x_2} & \frac{x_2}{w_{X2}+x_2} & \frac{y_2}{w_{X2}+x_2} \\ \frac{x_1}{w_{Y2}+y_2} & \frac{y_1}{w_{Y2}+y_2} & \frac{x_2}{w_{Y2}+y_2} & \frac{y_2}{w_{Y2}+y_2} \end{bmatrix} \tag{5}$$

$$\boldsymbol{S}(j\omega) = \begin{bmatrix} \frac{w_{X1}+x_1}{w_{X1}} & \frac{y_1}{w_{X1}} & \frac{x_2}{w_{X1}} & \frac{y_2}{w_{X1}} \\ \frac{x_1}{w_{Y1}} & \frac{w_{YL}+y_1}{w_{Y1}} & \frac{x_2}{w_{Y1}} & \frac{y_2}{w_{Y1}} \\ \frac{x_1}{w_{X2}} & \frac{y_1}{w_{X2}} & \frac{w_{XR}+x_2}{w_{X2}} & \frac{y_2}{w_{X2}} \\ \frac{x_1}{w_{Y2}} & \frac{y_1}{w_{Y2}} & \frac{x_2}{w_{Y2}} & \frac{w_{Y2}+y_2}{w_{Y2}} \end{bmatrix} \tag{6}$$

In case that sensitivity function matrix $\boldsymbol{S}(j\omega)$ is measured in MIMO, the stability margin distance $L_{ss}$ may be expressed as follows:

$$\begin{aligned} &L_{ss} = \frac{1}{S_{\max}}, S_{\max} = \max_{\omega}\left\{\max_{i,j}\left[\left|S_{ij}(j\omega)\right|\right]\right\} \\ &\boldsymbol{S}(j\omega) = \left[S_{ij}(j\omega)\right], (\ i,j = 1\cdots 4) \end{aligned} \tag{7}$$

According to ISO/FDIS-14839-3 as mentioned before, the stability index is defined as follows:

$$\text{Peak sensitivity} = 20\log S_{\max}$$

$$S_{\max} = \max_{\omega}\left\{\max_{i,j}\left[\left|S_{ij}(j\omega)\right|\right]\right\} \tag{8}$$

$$\boldsymbol{S}(j\omega) = \left[S_{ij}(j\omega)\right],\ (i,j = 1\cdots 4)$$

In addition to $L_{ss}$, the stability margin distance $L_{sg}$ drawn from the maximum singular value $\sigma_{\max}(j\omega)$ of the sensitivity function matrix $\boldsymbol{S}(j\omega)$ is defined as follows:

$$L_{sg} = \frac{1}{\overline{\sigma}}, \overline{\sigma} = \max_{\omega}\{\sigma_{\max}(j\omega)\} \tag{9}$$

, where $L$ is a dimensionless number. This is because both inputs and outputs are displacement signals when the sensitivity functions are estimated.

Whenever we examine an occurrence of self-excited vibration in rotating machinery using sliding bearings such as oil whip, steam whirl and so on, complex eigen values of rotor system are analyzed and the sign and the magnitude of their real parts of is referred as an index of the occurrence of self-excited vibration. Therefore, we adopt damping ratio $\zeta$ of the natural vibration of the rotor as an index and compare with the above-mentioned index here. Since the damping ratio of a flexible rotor is the order of 0.01, the value $10\zeta$ which is ten times of the damping ratio is adopted for comparing the above mentioned indexes.

## Ⅳ. EXPERIMENTAL TEST RIG

In order to investigate how the five above-mentioned stability margin distances change when the stability of the control system changes and the state where an unstable oscillation occurs on a rotor is approached, we have manufactured a small test rotor apparatus levitated by magnetic bearings. Figure 3 shows a photograph of the test apparatus.

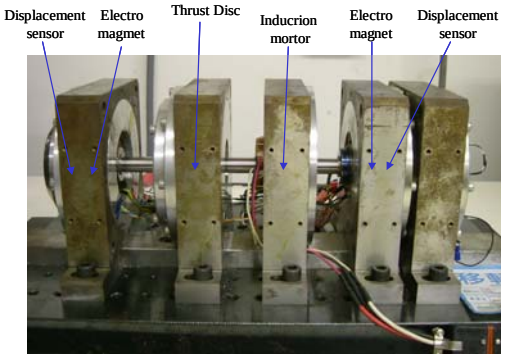


Figure3 Photograph of tested rotor-AMB system

Figure4 shows a sectional diagram of the rotor supported by AMB, of which controllers are constituted of PID and notch filter for eliminating higher bending mode natural vibration of the rotor.

The rotor is about 12mm in diameter and 300mm in length. Its 1st and 2nd natural frequencies are about 420Hz and 1200Hz in standstill.

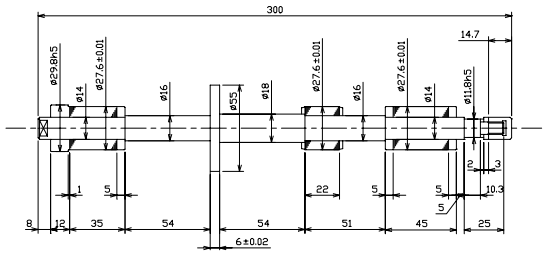


Figure 4 Shape of rotor

The electric circuit diagram and the original Bode diagram of the PID circuit are shown in Figure 5 and Figure 6.
The central frequency of the notch filter is about 3000Hz.

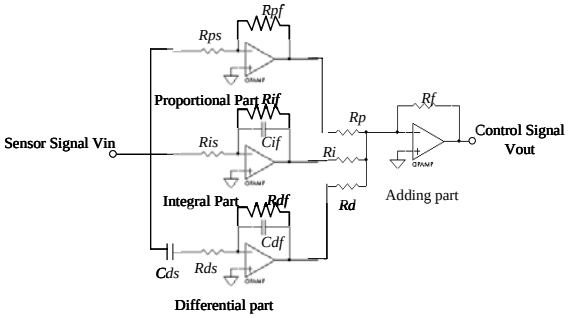


Figure 5 PID Controller

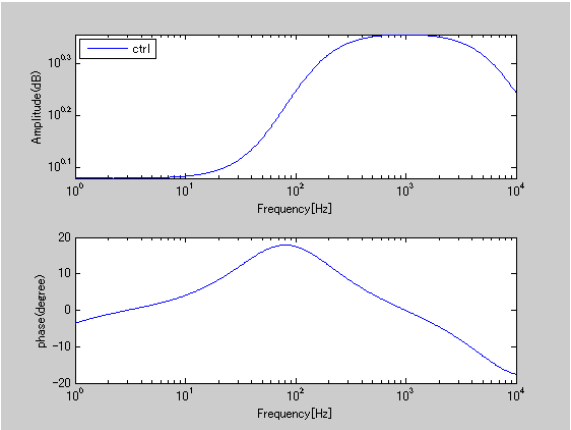


Figure 6 Bode diagram of PID controller

In order to estimate the stability indexes using the test apparatus, we have carried out a series of experiments by adjusting the proportional and differential gains $R_p, R_d$ in Figure 5, and changing the system stability into unstable condition and measured the open-loop transfer functions and the sensitivity functions by using a servo analyser (NF Corp. 5050).

## Ⅴ. EXPERIMENTAL RESULTS

Figure 7 shows 16 Bode diagrams of the open loop transfer function of the rotor-AMB system as 4 inputs and 4 outputs MIMO system using the original

parameters $(R_P = 20k, R_d = 20k)$, $(k_P = 1.2, k_d = 0.0015)$ for the controller and at the rated speed 12000rpm.
(The phase lead diagrams which indicate about 0 degree at 1 Hz should be shifted to -180 degree.)

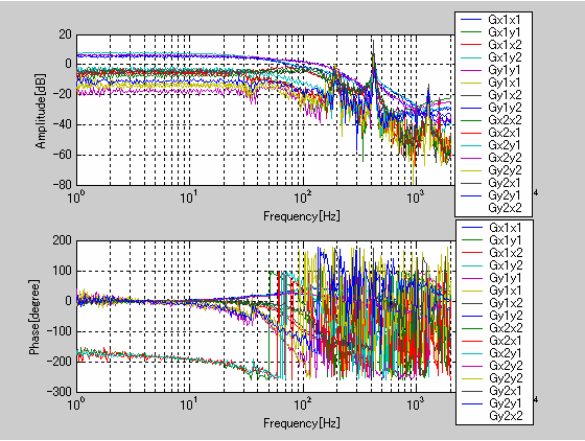

Figure 7 Open loop transfer function

The peak frequencies 200Hz, 420Hz and 1200Hz in the Bode diagram are corresponding with the rotating speed, the 1st bending natural frequency and the 2nd bending natural frequency; therefore we should neglect the peak gain at 200Hz in consideration of the system stability.
Since it is complicated to distinguish16 curves in the transfer matrix at the same diagram, we draw 4 open loop transfer functions concerning the output $x_1$ in Figure 8.
The peak gains of the diagonal term in the transfer function matrix of the open loop are larger than 0dB. The gains of the non-diagonal terms at each frequency are smaller than the diagonal terms.
The curves for the phase lag of the non-diagonal term of the transfer function matrix show decrease gradually with frequency.

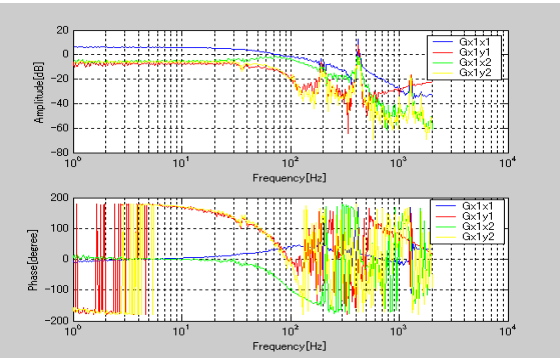

Figure 8 Open loop transfer functions related output $x_1$

Next, we show four transfer functions of the diagonal component of the matrix in Figure 9.
The figure shows that the transfer function of the diagonal term has a phase lead by about 100Hz. It can be checked from this that a countermeasure has been taken against the unstable phenomenon in the rigid-body mode of the rotor with the PID controller. We can see that the peak gain at the 1st natural frequency 420Hz is sharp and about 15dB.
On the other hand, the peak gain at the 2nd natural frequency1200Hz is sharp but under -10dB and then the control system does not come up against the instability of the natural vibration.

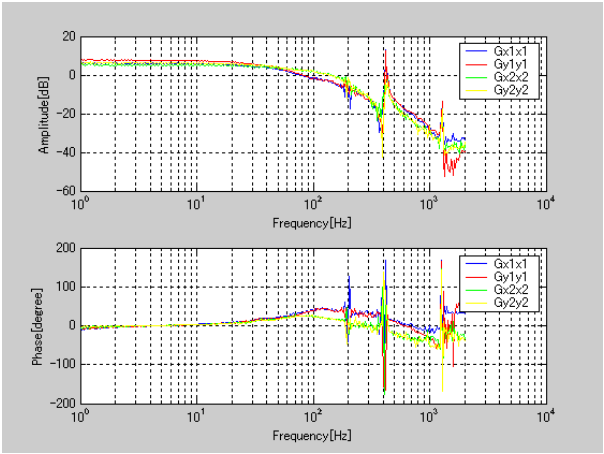

Figure 9 Diagonal term of transfer function matrix of open-loop (original controller)

Figure 10 shows polar plots of the open-loop transfer functions of the system using the original controller drawn on the Gauss plane. The figure is zoomed in to make the change of the locus clear near the origin. Therefore, the locus near the 1st natural frequency becomes larger and is pushed out. The figure shows that every locus of the open-loop transfer function encircles the critical point $(-1, j0)$ in the counter-clockwise as $\omega$ varies from 0 to $\infty$ , and the control system is stable.

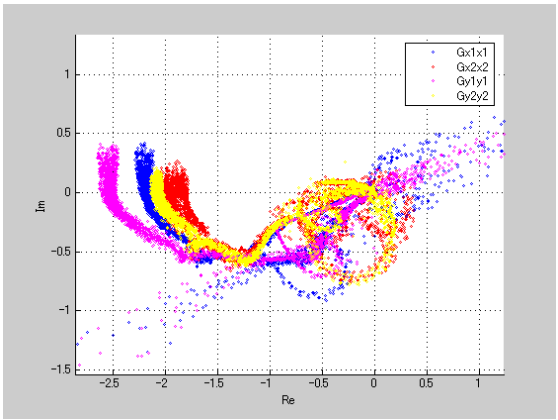

Figure 10 Nyquist plot of diagonal term of open-loop transfer function matrix (original controller)

Next, 16 sensitivity functions contained in the sensitivity function matrix of a dimension $4 \times 4$ are calculated from the open-loop transfer functions and are displayed on Figure 11in case of changing the proportional gain to a half of the original value. As mentioned before, we neglect the peak gain at 200Hz because it is a component of the rotating speed.
The gain of the sensitivity function becomes maximum value at the 1st bending natural frequency 420Hz and maximum gain of $S_{x1x1}$ is 4dB, but the maximum gain of

the sensitivity function near the 2nd natural frequency is 1dB and then the effect of the 2nd natural vibration on the system stability may be neglected.
The figure also shows that the gain of non-diagonal terms is smaller than that of the diagonal terms.

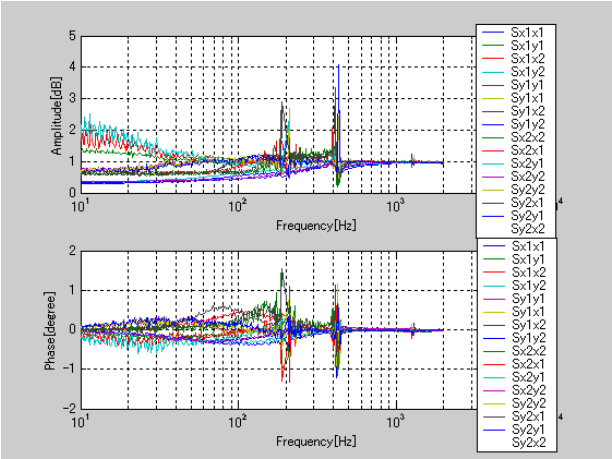


Figure 11 Bode diagram of sensitivity function matrix
( $K_d = 1.5 \times 10^{-3}$, $K_p = 0.96$ )

Figure 12 shows the maximum gain among 16 gains of the sensitivity function matrix at each frequency. The figure also shows that the gain becomes maximum value at the 1st bending natural frequency 420Hz and is 4.1dB, but the peak gain near the 2nd natural frequency 1200Hz is 1.2dB.

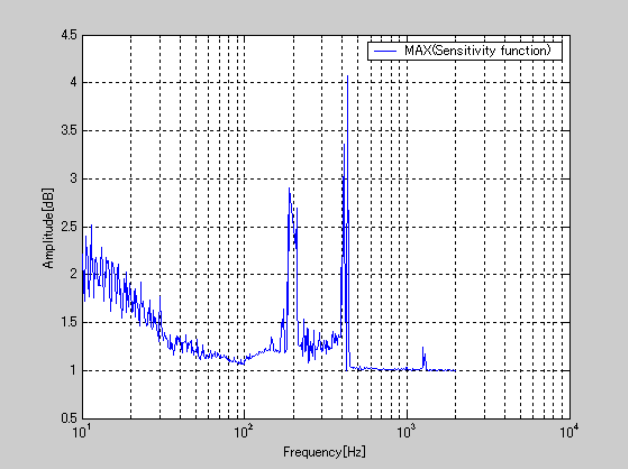


Figure 12 Maximum gain of sensitivity function
( $K_d = 1.5 \times 10^{-3}$, $K_p = 0.96$ )

Next, the four singular values of the $4 \times 4$ sensitivity function matrix have been calculated for every frequency and they are plotted on Figure 13.
The Maximum singular value among 4 singular values for every frequency spreads between 2.5dB and 5.3dB. The maximum value among them is 5.3dB and its corresponding frequency is the 1st natural frequency.
Accordingly, the maximum value of the singular values is larger than the maximum gain of the sensitivity functions and the difference of the maximum value between the singular values and the gain of the sensitivity functions is $5.3 - 4.1 = 1.2\text{dB}$ .

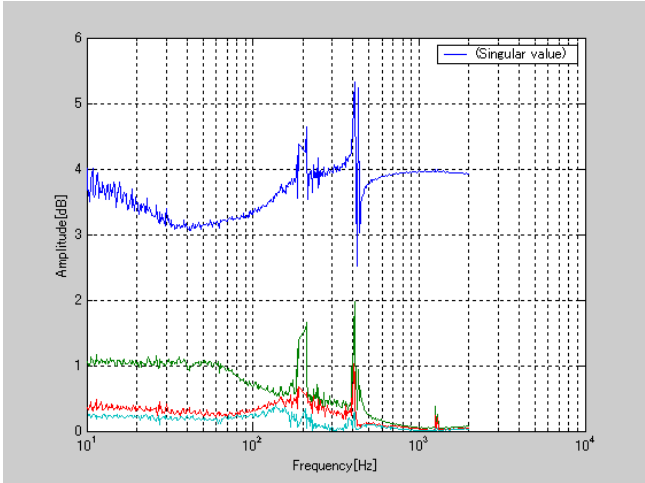


Figure 13 Singular value of sensitivity function
( $K_d = 1.5 \times 10^{-3}$, $K_p = 0.96$ )

In order to change the stability of the tested small rotor-AMB system, the proportional gain and differential gain of the PID controller were changed. At this time, the stability margin distances $L_{gm}, L_{pm}, L_{ss}, L_{sg}$ and damping ratio were measured. Ten times of the damping ratio $10\zeta$ is used for comparison among them. The measured results are shown in Figure 14 and Figure 15.
The proportional gain $k_p$ is changed between 0.68 and 1.85 . The differential gain $k_d$ is changed between $0.75 \times 10^{-3}$ and $2.6 \times 10^{-3}$ .
When the change of the control gain was set to be beyond the before-mentioned range of the gain, an occurrence of the system instability was observed.
As shown in Figure 14, in case that the proportional gain is changed, $L_{pm}$ is largest among 4 stability margin distances and the indicated distance becomes smaller in order of $L_{gm}, L_{pm}, L_{ss}$ .
The stability margin distance $L_{sg}$ given by the maximum singular value can be calculated between $k_p = 0.68$ and $k_p = 1.2$ , but it can't be calculated beyond $k_p = 1.2$ because of noise in the measured data.
The damping ratio ( $10\zeta$ ) keeps almost constant in changing the proportional gain $k_p$ .
When the gain is increased and becomes over 1.4 , $L_{ss}$ reaches under 0.2. But the control system does not get unstable and can be operated, although the stability margin distance 0.2 corresponds to the trip boundary C/D in ISO.
When the differential gain $k_d$ is changed, $L_{pm}$ is also largest among 4 stability margin distances and the indicated distance becomes smaller in order of $L_{gm}, L_{pm}, L_{ss}$ as shown in Figure 15.

Decreasing $k_d$ , the control system approaches unstable condition, and then $L_{gm}$ and $L_{pm}$ decreases rapidly. Especially the change of $L_{gm}$ is large. At same time, the damping ratio reaches to zero.

In this case, the changes in $L_{gm}$ , $L_{pm}$ and $L_{ss}$ is larger than $10\zeta$ .

From these experimental results, we confirm that $L_{gm}$ , $L_{pm}$ and $L_{ss}$ are more suitable than $10\zeta$ and $L_{sg}$ for judging the stability of rotor-AMB systems.

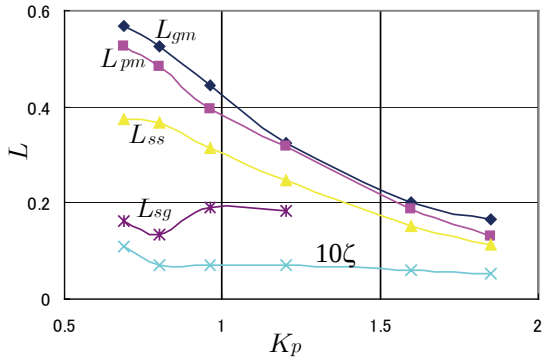


Figure 14 Experimental result for estimating the criteria in case that the proportional gain is changed among $k_p = 0.68$ and $k_p = 1.85$ .

## VI. CONCLUSIONS

In this paper, a series of experimental studies have been carried on the stability margin of rotor-AMB system and following results are obtained:

As an index by which the stability margin of a rotor-magnetic bearing system is evaluated, stability margin distance was defined and a series of experiments was carried out for comparison among the gain margin, the phase margin, the maximum gain of sensitivity function, the maximum singular value of sensitivity function matrix, and the damping ratio using the stability margin distance, and the following conclusions were obtained:

(1) $L_{gm}$ , $L_{pm}$ and $L_{ss}$ show changes with the almost same tendency to change of the control gain and the stability of the rotor-AMB system.

(2) The change of $\zeta$ shows a different tendency to change of the control gain. Therefore, the damping ratio is unsuitable for judging the system stability.

(3) Though $L_{ss}$ becomes under 0.2, which corresponds to factor 5 and 14dB the trip boundary C/D in ISO, the control system does not get unstable and can be operated.

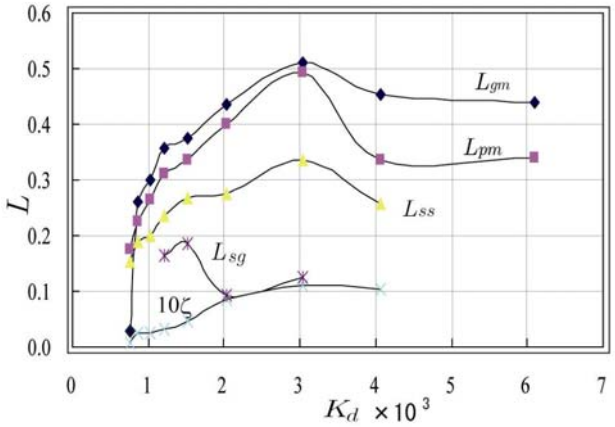


Figure 15 Experimental results for estimating the criteria in case that the differential gain is changed among $k_d = 0.76\times10^{-3}$ and $4.06\times10^{-3}$ .

## REFERENCES


[1] Kanemitsu,Y, et al., Japanese proposal for International standardization for active magnetic bearing , Proc. 5th International Symposium on Magnetic Bearings pp.265-270 (1996)

[2] Matsushita,O., et al., Standardization of evaluation of stability margin for active magnetic bearing equipped rotors, Proc.ImechE2000, pp.361-370 (2000)

[3] ISO-DIS-14839-3 Mechanical vibration -- Vibration of rotating machinery equipped with active magnetic bearings – Part 3: Evaluation of stability margin (2004)

[4] Kanemitsu,Y., et al, Analytical comparison of stability criteria for rotor levitated by active magnetic bearing, Proc. 11th Asia-Pacific Vibration Conference,pp.337-343(2005)